

The Catalytic Carboxyester Hydrolysis by a New Zinc(II) Complex with an Alcohol-Pendant Cyclen
(1-(2-Hydroxyethyl)-1,4,7,10-tetraazacyclododecane): A Novel Model for Indirect Activation of the Serine Nucleophile by Zinc(II) in Zinc Enzymes

Tohru Koike,[†] Satoko Kajitani,[†] Ikushi Nakamura,[†] Eiichi Kimura,^{*,†} and Motoo Shiro[‡]

Contribution from the Department of Medicinal Chemistry, School of Medicine, Hiroshima University, Kasumi 1-2-3, Minami-ku, Hiroshima 734, Japan, and Rigaku Corporation, Matsubaracho 3-9-12, Akishima, Tokyo 196, Japan

Received September 6, 1994[⊗]

Abstract: A new macrocyclic tetraamine (cyclen) having a strategically appended alcohol group, 1-(2-hydroxyethyl)-1,4,7,10-tetraazacyclododecane (**8**), has been synthesized. The functionalized cyclen (**8**) forms a 1:1 ZnL complex (**5**) at pH ca. 6. The X-ray crystal study has disclosed a five-coordinate structure with the undeprotonated alcohol OH coordinating at an apical position. Crystals of **5**·(ClO₄)₂ (C₁₀H₂₄N₄O₉Cl₂Zn) are monoclinic, space group *P*2₁/*n* with *a* = 8.813 (2) Å, *b* = 23.662 (2) Å, *c* = 8.814 (2) Å, β = 90.21 (1)°, *V* = 1838.0 (5) Å³, *Z* = 4, *R* = 0.073, and *R*_w = 0.125. The potentiometric pH titration of **5** showed dissociation of a proton with a p*K*_a value of 7.60 ± 0.02 at 25 °C and *I* = 0.10 (NaClO₄). From the NMR and competitive anion-binding studies, the structure of the deprotonated species was assigned to be a OH⁻-bound ZnL–OH⁻ complex (**11**). During unsuccessful attempts to isolate the deprotonated species, we have obtained a trimeric phosphate complex, (ZnL–O–)₃P=O, as its PF₆⁻ salts (**15**·(PF₆)₃(H₂O)_{1.5}) from pH 9.5 aqueous solution containing **5**·(ClO₄)₂, K₂HPO₄, and NH₄PF₆. Crystals of **15**·(PF₆)₃(H₂O)_{1.5} (determined as the trimer of C₁₀H₂₅N₄O_{17/6}P_{4/3}F₆Zn) are trigonal, space group *R*3̄ with *a* = 23.353 (3) Å, *c* = 17.527 (5) Å, *V* = 8278 (2) Å³, *Z* = 18, *R* = 0.070, and *R*_w = 0.112. Among the known Zn^{II} complexes, the ZnL–OH⁻ complex **11** is the most active catalyst for 4-nitrophenyl acetate (NA) hydrolysis. In the kinetic studies using **5** in 10% (v/v) CH₃CN at 25 °C, *I* = 0.10 (NaNO₃), and pH 6.4–9.5, the pH-rate profile gave a sigmoidal curve with an inflection point at pH 7.7, which corresponds to the p*K*_a value for ZnL (**5**) ⇌ ZnL–OH⁻ (**11**) + H⁺. The second-order (first-order each in [**11**] and [NA]) rate constant of 0.46 ± 0.01 M⁻¹ s⁻¹ is approximately ten times greater than the corresponding value of (4.7 ± 0.1) × 10⁻² M⁻¹ s⁻¹ for *N*-methylcyclen–Zn^{II}–OH⁻ complex **12b** catalyst. Furthermore, we found the NA hydrolysis to occur through a double-displacement reaction of the acetyl group. In the first rate-determining reaction, the nucleophile is the pendant alcoholic OH “activated” by the adjacent Zn^{II}–OH⁻, which attacks NA to yield an “acyl intermediate” (**16**). This intermediate was independently synthesized by the reaction of **5** with acetic anhydride in CH₃CN. In the second reaction, **16** is subject to extremely fast hydrolysis (e.g., *t*_{1/2} = 6 s at pH 9.3), as monitored on spectral change of pH-indicators. A plot of the observed first-order rate constants against pH (=6.1–9.3) for the second process gave a sigmoidal curve with its inflection point at pH 7.7, which is a similar value for the p*K*_a's of the Zn^{II}–cyclen complexes **4a** and **12a**. It is concluded that the very fast second reaction occurs through the nucleophilic attack of the Zn^{II}–OH⁻ (**16a**) at the intramolecular acetyl group. The overall NA hydrolysis by **11** is catalytic. Thus, the OH⁻-bound ZnL plays dual roles: as a general base in the first acyl-transfer reaction to activate the remote alcoholic OH and as a nucleophile to attack the electrophilic center in the second hydrolysis step. Such a dyad of Zn^{II}–OH⁻ and the adjacent alcoholic OH may account for the strong nucleophilicity of serine at the active center of zinc enzymes such as alkaline phosphatase.

Introduction

Hydrolytic enzymes often use external H₂O or internal alcoholic residues (e.g., serine, threonine) as nucleophiles to react with electrophilic substrates (carboxyesters, phosphates, and amides), wherein the prior activation of the nucleophiles (and/or the electrophiles) is essential.¹ For instance, in carbonic anhydrase (CA) the Zn^{II}-bound water at the active center deprotonates to yield the good nucleophile Zn^{II}-OH⁻ which attacks the electrophilic center of the substrate CO₂ (Scheme 1).² In chymotrypsin (a “serine” enzyme), the alcoholic OH

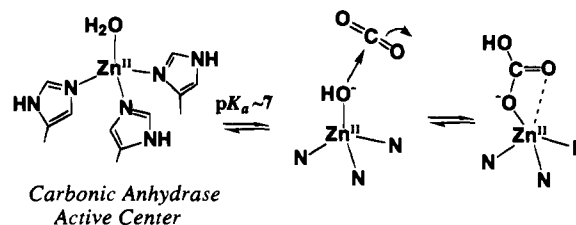
[†] Hiroshima University.

[‡] Rigaku Corporation.

[⊗] Abstract published in *Advance ACS Abstracts*, January 1, 1995.

(1) Book reviews: (a) *Hydrolytic Enzymes*; Neuberger, A., Brocklehurst, K., Eds.; Elsevier Science: Amsterdam, 1987. (b) *Zinc Enzymes*; Bertini, I., Luchinat, C., Maret, W., Zeppeauer, M., Eds.; Birkhäuser: Boston, 1986.

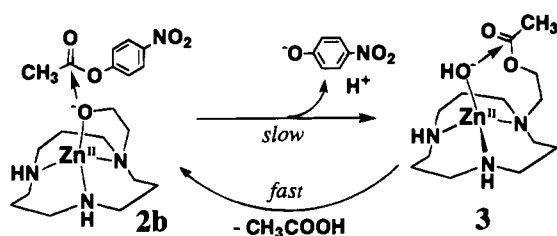
Scheme 1



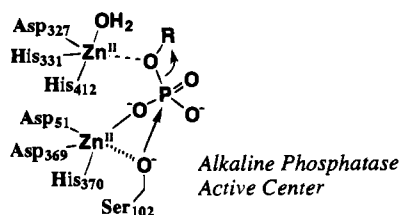
(Ser₁₉₅) is an initial nucleophile activated by an adjacent imidazole (His₅₇), which yields an “acyl-intermediate”.^{1,3} In the second reaction, water is activated by the same imidazole to attack the “acyl-intermediate” to recycle the hydrolysis.

In our earlier zinc enzyme model studies using 1,5,9-triazacyclododecane ([12]aneN₃)–Zn^{II} complex (**1**),^{4,5} we showed

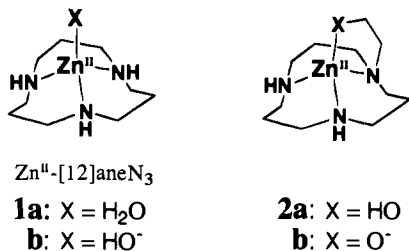
Scheme 2



Scheme 3



that a water bound to Zn^{II} at the fourth coordination site is activated (i.e., its pK_a value for $ZnL-OH_2$ (**1a**) \rightleftharpoons $ZnL-OH^-$ (**1b**) is 7.3 at 25 °C), probably in a way similar to that of CA, to catalyze CO_2 hydration and ester hydrolysis. We then synthesized an alcohol-pendant [12]ane N_3 - Zn^{II} complex (**2**).⁶ The tethered alcoholic OH of **2a** deprotonates with pK_a value of 7.4 to yield an alkoxide RO^- - Zn^{II} complex (**2b**), whose dimeric structure was proven by the X-ray crystal analysis, NMR, and potentiometric pH titration studies. In 4-nitrophenyl acetate (NA) hydrolysis by **2b** this Zn^{II} -bound alkoxide anion directly attacked at the electrophilic ester carbonyl to yield an acyl-intermediate (**3**) (see Scheme 2), which is then very quickly hydrolyzed possibly by the intramolecular Zn^{II} -bound H_2O (or OH^-) to complete the hydrolysis and regenerate the initial alkoxide complex **2b**. The double displacement of the acyl group by **2b** reminded us of the proposed hydrolysis mechanism by alkaline phosphatase (see Scheme 3).⁷ The role of Zn^{II} in the activation of the proximate alcoholic OH may be common in both the natural⁷ and model cases.^{6,8} However, the detailed mechanism of the double displacement reaction had yet to remain elucidated. The instability of **2b** and the acyl intermediate **3** in wide range of pH in aqueous solution hindered more extensive investigation, such as pH-dependent kinetics.



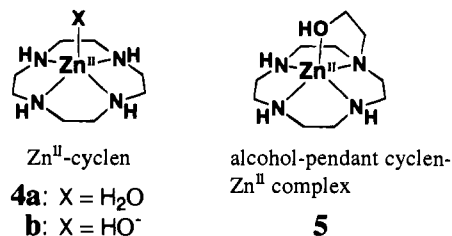
Recently, we have demonstrated that Zn^{II} complex (**4**) of 1,4,7,10-tetraazacyclododecane (cyclen) is a functional model

(2) *Carbonic Anhydrase*; Botrè, F., Gros, G., Storey, B. T., Eds.; VCH: New York, 1990.

(3) (a) Blow, D. M.; Birktoft, J. J.; Hartley, B. S. *Nature* **1969**, *221*, 337–340. (b) Dugas, H. *Bioorganic Chemistry*; Springer-Verlag: New York, 1989; p 196. (c) Frey, P. A.; Whitt, S. A.; Tobin, J. B. *Science* **1994**, *264*, 1927–1930.

(4) (a) Kimura, E.; Shioita, T.; Koike, T.; Shiro, M.; Kodama, M. *J. Am. Chem. Soc.* **1990**, *112*, 5805–5811. (b) Zhang, X.; van Eldik, R.; Koike, T.; Kimura, E. *Inorg. Chem.* **1993**, *32*, 5749–5755. (c) Kimura, E.; Koike, T.; Shionoya, M.; Shiro, M. *Chem. Lett.* **1992**, 787–790. (d) Koike, T.; Kimura, E. *J. Am. Chem. Soc.* **1991**, *113*, 8935–8941. (e) Koike, T.; Kimura, E.; Nakamura, I.; Hashimoto, Y.; Shiro, M. *J. Am. Chem. Soc.* **1992**, *114*, 7338–7345. (f) Kimura, E.; Shionoya, M.; Hoshino, A.; Ikeda, T.; Yamada, Y. *J. Am. Chem. Soc.* **1992**, *114*, 10134–10137.

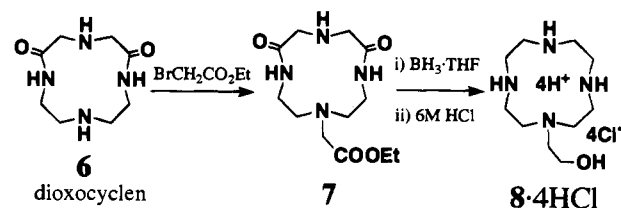
for a zinc-containing hydrolytic enzyme, β -lactamase II.⁹ The water bound to the Zn^{II} at the apical site is also activated with the pK_a value of 7.9 for **4a** \rightleftharpoons **4b**. A great advantage of the tetraamine [12]ane N_4 (cyclen) over the triamine [12]ane N_3 was that the Zn^{II} ion is more firmly held, which allowed us to study the behavior of ligands (X) in the wide range of pH without worry about degradation of the Zn^{II} -macrocylic complex part. Accordingly, we designed an alcohol-pendant cyclen- Zn^{II} complex (**5**) in order to further investigate the activation mechanism of the alcohols in Zn^{II} enzymes and also to seek for better and more practical hydrolytic catalyst.¹⁰ In the present experiments with **5**, we have discovered a more insightful picture of the Zn^{II} activation of the proximate alcohol, which is more instructive for the zinc enzyme mechanism than the previous model by **2**. We also have found **5** to be the most efficient catalyst for 4-nitrophenyl acetate hydrolysis among all the Zn^{II} complexes studied so far.



Results and Discussion

Synthesis of 1-(2-Hydroxyethyl)-1,4,7,10-tetraazacyclododecane (Alcohol-Pendant Cyclen), **8 (Scheme 4).** The macrocyclic dioxotetraamine (**6**)¹¹ was treated with ethyl bromoacetate in DMF at room temperature for 3 h to obtain 10-((ethoxycarbonyl)methyl)-2,6-dioxo-1,4,7,10-tetraazacyclododecane **7** in 63% yield. All the carbonyl groups were reduced with $BH_3 \cdot THF$ complex in THF to give the desired product 1-(2-hydroxyethyl)-1,4,7,10-tetraazacyclododecane **8**, which was purified as its tetrahydrochloride salts from 6 M aqueous HCl solution in 66% yield.

Scheme 4



(5) (a) Kimura, E.; Koike, T. *Comments Inorg. Chem.* **1991**, *11*, 285. (b) Kimura, E. *Progress in Inorganic Chemistry*; Karlin, K. D., Ed.; John Wiley & Sons: 1994; Vol. 41, p 443.

(6) Kimura, E.; Nakamura, I.; Koike, T.; Shionoya, M.; Kodama, Y.; Ikeda, T.; Shiro, M. *J. Am. Chem. Soc.* **1994**, *116*, 4764–4771.

(7) (a) Coleman, J. E. *Annu. Rev. Biophys. Biomol. Struct.* **1992**, *21*, 441–483. (b) Kim, E. E.; Wyckoff, H. W. *J. Mol. Biol.* **1991**, *218*, 449–464. (c) Butler-Ransohoff, J. E.; Rokita, S. E.; Kendal, D. A.; Banzon, J. A.; Carano, K. S.; Kaiser, E. T.; Matlin, A. R. *J. Org. Chem.* **1992**, *57*, 142–145.

(8) (a) Sigman, D. S.; Jorgensen, C. T. *J. Am. Chem. Soc.* **1972**, *94*, 1724–1731. (b) Gellman, S. H.; Petter, R.; Breslow, R. *J. Am. Chem. Soc.* **1986**, *108*, 2388–2394. (c) Herschlag, D.; Jencks, W. P. *J. Am. Chem. Soc.* **1987**, *109*, 4665–4674. (d) Clewley, R. G.; Slebocka-Tilk, H.; Brown, R. S. *Inorg. Chim. Acta* **1989**, *157*, 223–238. (e) Weijnen, J. G. J.; Koudijs, A.; Engbersen, J. F. J. *J. Org. Chem.* **1992**, *57*, 7258–7265.

(9) Koike, T.; Takamura, M.; Kimura, E. *J. Am. Chem. Soc.* **1994**, *116*, 8443–8449.

(10) (a) Chin, J.; Banaszczuk, M.; Jubian, V.; Kim, J. H.; Mrejen, K. *Bioorganic Chemistry Frontiers*; Dugas, H., Ed.; Springer-Verlag: Berlin, 1991; Vol. 2, p 176. (b) Suh, J. *Acc. Chem. Res.* **1992**, *25*, 273–279. (c) Hendry, P.; Sargeson, A. M. *Progress Inorg. Chem.: Bioinorg. Chem.* **1990**, *38*, 201–258.

(11) Kimura, E.; Kuramoto, Y.; Koike, T.; Fujioka, H.; Kodama, M. *J. Org. Chem.* **1990**, *55*, 42–46.

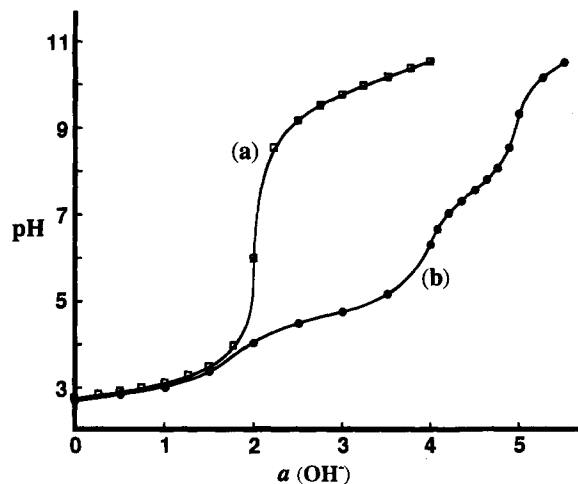


Figure 1. Typical titration curves for **8**·4HCl at 25 °C and $I = 0.10$ (NaClO_4): (a) 1.0 mM of **8**·4HCl; (b) a + 1.0 mM for ZnSO_4 (or $5 \cdot (\text{ClO}_4)_2 + 4.0$ mM HCl).

Table 1. Comparison of the Protonation Constants of the Cyclen and Alcohol-Pendant Cyclen (**8**), Zn^{II} Complexation Constants, and Deprotonation Constants of Zn^{II} -Bound Water^a

	cyclen	8
$\log K_1$	11.04 ± 0.05^b	10.72 ± 0.05^b
$\log K_2$	9.86 ± 0.03^b	9.28 ± 0.03^b
$\log K_3$	$<2^b$	$<2^b$
$\log K_4$	$<2^b$	$<2^b$
$\log K(\text{ZnL})$	15.3 ± 0.1^c (16.2) ^d	13.8 ± 0.1^f
$\text{p}K_a$		
15 °C	8.06^d	7.78 ± 0.02^g
25 °C	7.86^e	7.60 ± 0.02^g (7.70 ± 0.03) ^h
35 °C	7.64^e	7.41 ± 0.02^g

^a $K_n = [\text{H}_n\text{L}]/[\text{H}_{n-1}\text{L}]a_{\text{H}^+}$. $K(\text{ZnL}) = [\text{ZnL}]/[\text{L}][\text{Zn}^{\text{II}}]$. $K_a = [\text{ZnL-OH}^-]a_{\text{H}^+}/[\text{ZnL}]$. ^b At $I = 0.10$ (NaClO_4) and 25 °C. ^c Determined with 1.0 and 2.0 mM of **4a**·(ClO_4)₂·H₂O and 4 equiv of HClO₄ at $I = 0.10$ (NaClO_4) and 25 °C. ^d From ref 12. Determined by polarographic method at 25 °C, $I = 0.2$ (acetate buffer) and pH = 4–5. ^e From ref 9. ^f Determined with 1.0 and 2.0 mM of **5** and 4 equiv amount of HClO₄ at $I = 0.10$ (NaClO_4) and 25 °C. ^g Determined with 0.5, 1.0, and 2.0 mM of **5** at $I = 0.10$ (NaClO_4). ^h Determined with 1.0 and 2.0 mM of **5** at $I = 0.10$ (NaNO_3) in 10% (v/v) CH₃CN.

Protonation and Zinc(II) Complexation Constants of Alcohol-Pendant Cyclen (8**).** The protonation constants (K_n) of **8** were determined by potentiometric pH titrations of **8**·4HCl (1 mM) with 0.10 M NaOH at $I = 0.10$ (NaClO_4). A typical pH titration curve for **8**·4HCl at 25 °C is shown in Figure 1a. The titration data were analyzed for equilibria 1–4. The mixed protonation constants K_1 – K_4 (a_{H^+} is the activity of H^+) are defined as follows

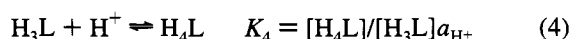
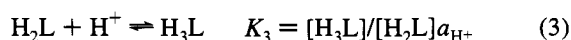
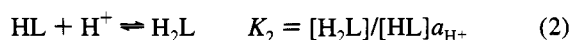
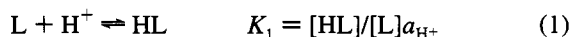


Table 1 summarizes the obtained protonation constants ($\log K_n$) in comparison with the K_n values of cyclen under the same conditions. The K_1 and K_2 values of **8** are extremely large with respect to K_3 and K_4 values, which are roughly the same as those of cyclen.

The potentiometric pH titration curve of **8**·4HCl in the presence of equimolar amount of Zn^{II} with 0.10 M NaOH (Figure 1b) revealed complex formation at $4 < \text{pH} < 6$, followed by the dissociation of one equivalent proton, as shown by two

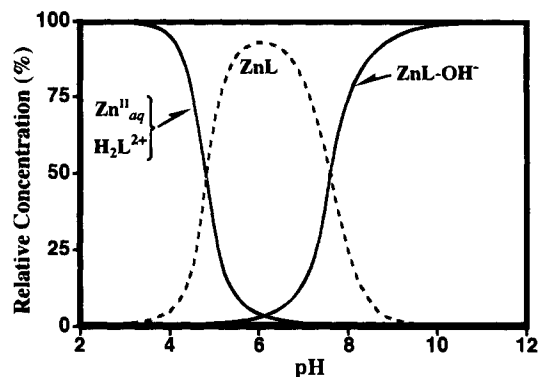
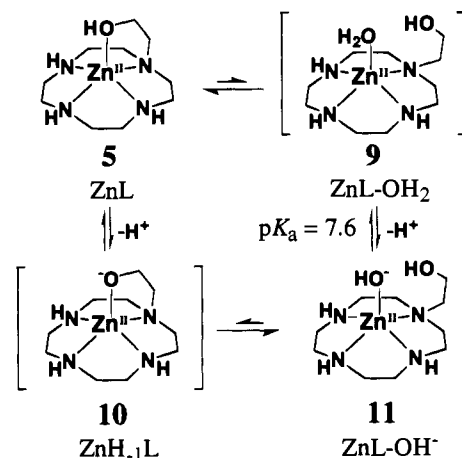
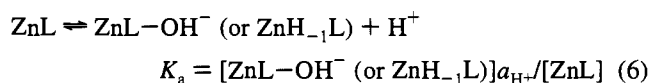
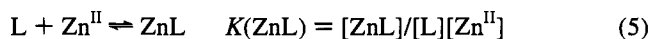


Figure 2. Distribution diagram for 1 mM Zn^{II} /1 mM **8**·4HCl system as a function of pH at 25 °C and $I = 0.10$ (NaClO_4): ZnL is **5**; ZnL-OH⁻ is the OH⁻-bound complex **11**.

Scheme 5

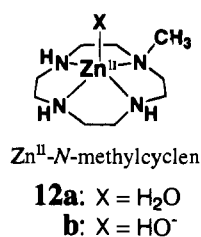


neutralization breaks at $a = 4$ and 5. Up to $a = 4$, the equilibration was extremely slow, so that we had to wait for more than 2 h at each titration point. The titration data were treated for the 1:1 ZnL complex (eq 5) and its monodeprotonated complex (eq 6). Any further deprotonation or precipitation of $\text{Zn}(\text{OH})_2$ was not observed over pH 12, indicating the stability of the monodeprotonated species. The 1:1 ZnL complex and the subsequent deprotonation mode can be drawn as shown by Scheme 5. For the 1:1 complex, either ZnL **5** or ZnL-OH₂ **9** may be assigned in aqueous solution. In solid state, the former structure **5** is disclosed by the following X-ray crystal analysis. For the monodeprotonated structure, either ZnH_{-1}L **10** or ZnL-OH^- **11** may be considered.



The obtained values $\log K(\text{ZnL})$ at 25 °C and the deprotonation constants ($\text{p}K_a$) for **4a** and **5** at 15, 25, and 35 °C are listed in Table 1. A typical distribution diagram for the alcohol-pendant cyclen system as a function of $-\log[\text{H}^+]$ at [total zinc] = [total alcohol-pendant cyclen] = 1 mM, 25 °C and $I = 0.10$ (NaClO_4) is displayed in Figure 2. It is found that although the stability of the ZnL complex **5** ($\log K = 13.8 \pm 0.1$ at 25 °C) is inferior to that of **4a** ($\log K = 15.3 \pm 0.1$),¹² **5** remains sufficiently stable at physiological pH. After formation of the N₄-macrocyclic complex completes at $a = 4$, the monodeprotonation occurs with a $\text{p}K_a$ value of 7.60 ± 0.02 at 25 °C. In the previous study on the triamine system **2**,⁶ the deprotonation

of the pendant alcoholic OH ($pK_a = 7.4$ at $25\text{ }^\circ\text{C}$) occurred simultaneously at the macrocyclic triamine Zn^{II} complexation. It is of interest to compare the value of 7.60 for **5** with the pK_a value of 7.86 at $25\text{ }^\circ\text{C}$ for the Zn^{II} -bound water at the fifth coordination site of **4a**.⁹ For another reference, the pK_a value of 7.68 (at $25\text{ }^\circ\text{C}$) for the Zn^{II} -bound water in the *N*-methylcyclen complex (**12a** \rightleftharpoons **12b**) is similar under the same conditions.¹³ We assign the deprotonated structure to be **11** rather than **10** by the following results.



X-ray Crystal Structure of the Zn^{II} Complex of Alcohol-Pendant Cyclen, **5.** The crystal structure has provided an unequivocal evidence for the structure of 1:1 ZnL complex **5**. Alcohol-*pendant* cyclen **8** (in acid-free form L, see Experimental Section) in EtOH was mixed with 1 equiv amount of $\text{Zn}^{\text{II}}(\text{ClO}_4)_2 \cdot 6\text{H}_2\text{O}$ at $60\text{ }^\circ\text{C}$. After the solvent was evaporated, the residue was recrystallized from an aqueous EtOH solution to obtain the 1:1 ZnL complex as colorless crystals. The elemental analysis (C, H, N) suggested the formula $\text{ZnL} \cdot (\text{ClO}_4)_2$ containing neither water nor EtOH. The crystal was subjected to X-ray structure analysis. Figure 3 shows an ORTEP drawing of **5**·(ClO_4)₂ with 30% probability thermal ellipsoids. Selected crystal data and collection parameters are displayed in Table 2.

The Zn^{II} ion lies above the four nitrogen atoms ($\text{N}_1, \text{N}_4, \text{N}_7, \text{N}_{10}$) of the cyclen and apically binds with the pendant (neutral) alcoholic oxygen O_{15} . The angles $\text{N}_1\text{-Zn-N}_7$ and $\text{N}_4\text{-Zn-N}_{10}$ are bent at 137.8 and 135.4° , respectively, indicating a distorted tetragonal-pyramidal structure. The zinc atom lies almost in the plane defined by $\text{N}_1, \text{N}_7,$ and O_{15} atoms (a total angle for $\text{N}_1\text{-Zn-N}_7, \text{N}_7\text{-Zn-O}_{15}$, and $\text{N}_1\text{-Zn-O}_{15}$ is 360.1°). The Zn-O_{15} bond distance of 1.994 \AA is shorter than the Zn-N bonds ($2.102\text{--}2.186\text{ \AA}$), despite O_{15} is a neutral OH. The present five-coordinate structure can be compared with the previous alkoxide-*pendant* macrocyclic triamine Zn^{II} complex

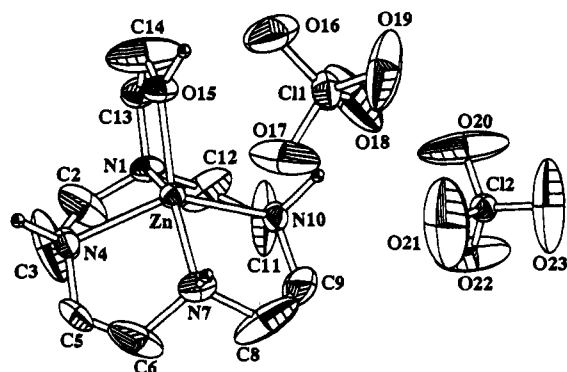
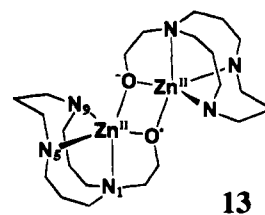


Figure 3. An ORTEP drawing (30% probability ellipsoids) of **5**·(ClO_4)₂. All hydrogen atoms bound to carbon are omitted for clarity: $\text{Zn-O}(15)$ 1.994 (4), $\text{Zn-N}(1)$ 2.186 (6), $\text{Zn-N}(4)$ 2.119 (5), $\text{Zn-N}(7)$ 2.102 (6), $\text{Zn-N}(10)$ 2.133 (5) \AA .

2b, which is a dimeric distorted trigonal-bipyramidal complex **13** bridged by the pendant alkoxide oxygens and has a much shorter coordinate Zn-O^- (alkoxide) bond of 1.95 \AA .⁶ The Zn-N bond lengths in **13** varies more widely ($\text{N}_5, 2.047$; $\text{N}_9, 2.067$; $\text{N}_1, 2.259\text{ \AA}$) than those in **5**. Although it is not inconceivable that in aqueous solution of **5** a water may replace the neutral alcohol pendant at the fifth coordination site to take an alternative structure **9**, we assume the structure **5** holding fairly firmly in aqueous solution, on the basis of the following results from ^1H NMR and anion binding studies.

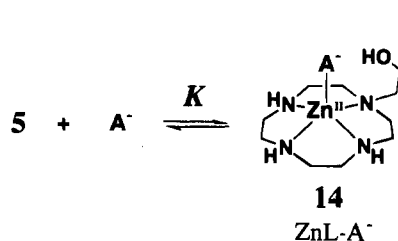


Anion Binding to the Zn^{II} Complex of Alcohol-Pendant Cyclen **5.** In Zn^{II} -cyclen complex **4a**, various anions (A^-) (e.g., CH_3COO^- , SCN^- , Cl^- , imide $^-$) can replace the H_2O at the axial site to yield 1:1 ZnL-A^- complexes.^{9,13} In order to see whether these anions (A^-) can replace the pendant alcohol

Table 2. Selected Crystallographic Data for **5** and the Monomeric Part of **15**·(PF_6)₃·(H_2O)_{1.5}

	5	15
empirical formula	$\text{C}_{10}\text{H}_{24}\text{N}_4\text{H}_9\text{Cl}_2\text{Zn}$	$\text{C}_{10}\text{H}_{25}\text{N}_4\text{O}_{17/6}\text{P}_{4/3}\text{F}_6\text{Zn}$
formula wt	480.6	467.4
crystal color, habit	colorless, prismatic	colorless, prismatic
crystal system	monoclinic	trigonal
space group	$P2_1/n$ (no. 14)	$R\bar{3}$ (no. 148)
lattice parameters	$a = 8.813(2)\text{ \AA}$ $b = 23.662(2)\text{ \AA}$ $c = 8.814(2)\text{ \AA}$ $\beta = 90.21(1)^\circ$ $V = 1838.0(5)\text{ \AA}^3$ $Z = 4$	$17.527(5)\text{ \AA}$ $8278(2)\text{ \AA}^3$ 18 36.77 cm^{-1}
$\mu(\text{Cu K}\alpha)$	50.32 cm^{-1}	
radiation	$\text{Cu K}\alpha$ ($\lambda = 1.54178\text{ \AA}$) graphite monochromated	
scan type	$\omega - 2\theta$	
scan rate (in ω)	$16.0^\circ/\text{min}$ (2 scans)	$16.0^\circ/\text{min}$ (5 scans)
scan width	$(1.89 + 0.30 \tan \theta)^\circ$	$(1.47 + 0.30 \tan \theta)^\circ$
$2\theta_{\text{max}}$	120.1°	109.8°
no. of reflns measd	total: 3004 unique: 2807 ($R_{\text{int}} = 0.027$)	total: 2506 unique: 2308 ($R_{\text{int}} = 0.067$)
refinement	full-matrix least squares	
function minimized	$\sum w(F_o - F_c)^2$	
least squares ws	$1/\sigma^2(F_o) = 4F_o^2/\sigma^2(F_c)$	
no. obsvns ($I > 3.00\sigma(I)$)	2438	1695
residuals: R, R_w	0.073, 0.125	0.070, 0.112

Scheme 6

**Table 3.** A Comparison of Anion Affinity Constants, $\log K$, for **5**, **4a**, and **12a** at 25 °C and $I = 0.10$ (NaClO₄)

anion	$\log K^a$		
	5	4a	12a
4-nitrophenyl phosphate ²⁻	3.0 ± 0.1 ^b	3.3 ± 0.1 ^b	3.3 ± 0.1 ^b
SCN ⁻	2.0 ± 0.1 ^c	2.2 ^d	2.4 ± 0.1 ^c
CH ₃ COO ⁻	1.6 ± 0.1 ^c	1.9 ^d	2.0 ± 0.1 ^c
Cl ⁻	1.3 ± 0.1 ^c	1.5 ^d	1.7 ± 0.1 ^c

^a $K = [\text{ZnL-A}^-]/[\text{ZnL}][\text{A}^-]$ (M⁻¹). ^b Determined with **2**, **5**, and 10 mM 4-nitrophenyl phosphate disodium salt and 1 mM ZnL. ^c Determined with 10, 20, and 50 mM corresponding sodium salt and 1 mM ZnL. ^d From ref 9.

(neutral) donor to yield ZnL-A⁻ complexes **14**, we have conducted the same potentiometric pH titration of ZnL **5** (and **12a** for reference) in the presence of 4-nitrophenyl phosphate²⁻, SCN⁻, CH₃COO⁻, and Cl⁻ anions at 25 °C; $I = 0.10$ (NaClO₄). The 1:1 anion affinity constants ($K = [\text{ZnL-A}^-]/[\text{ZnL}][\text{A}^-]$, M⁻¹, see Scheme 6) were calculated in the same fashion as previously described for cyclen-Zn^{II}-A⁻.⁹ All the $\log K$ values are listed in comparison with those corresponding values for **4a** and **12a** in Table 3. We see similar anion affinity constants among those cyclen complexes, which suggest that in **5** those anions replace the neutral alcohol OH and occupy the apical position like **4a** and **12a**. The *N*-methylcyclen complex **12a** has the highest A⁻ anion affinity for all of the anions tested (except for OH⁻), whereas the present *N*-hydroxyethyl cyclen complex **5** has the lowest affinity. Since the steric effect of the *N*-substituents on the apical position will not change much for **12a** and **5**, we concluded that there is a considerable competitive interaction of the alcohol OH with the Zn^{II} (supporting the structure **5**) in aqueous solution, which somewhat weakens the anion binding for **14**.

Can the OH⁻-bound complex **14** be depicted like **11** (ZnL-OH⁻) or equivalent alkoxide-bound **10** (ZnH₋₁L)? In order to settle which is correct, we have undertaken the differential ¹H NOE study of **5** (20 mM) in the presence of a large excess amount of anion (so as to form more than 95% 1:1 complexes on the basis of the anion affinity constant K) at 30 °C in D₂O. The results are summarized in Figure 4. Typical coupling constants and chemical shifts for alcohol-pendant cyclen-Zn^{II} complex are shown in the Experimental Section. At pD = 6.5 where as discussed above, the pendant OH is fixed to Zn^{II}, an intramolecular cross-relaxation for H_a (HC₁₄) → H_b (HC₁₃) (both on the pendant) was seen but not for H_a → H_c (HC of cyclen ring). However, at pD = 11 (so as to form completely monodeprotonated species **10** or **11**), a significant NOE appeared for H_a → H_c. Accordingly, we assign the ZnL-OH⁻ structure **11** (i.e., **14** (A⁻ = OH⁻)) at pD = 11, in which the free motion

(12) A $\log K(\text{ZnL})$ value of 16.2 for Zn^{II}-cyclen was previously determined by polarographic method at $I = 0.20$ (acetate buffer): Kodama, M.; Kimura, E. *J. Chem. Soc., Dalton Trans.* **1977**, 2269–2276. Due to the formation of CH₃COO⁻-Zn^{II}-cyclen complex (see $\log K$ value for the acetate complex in Table 4), the Zn^{II} complexation constant is over 10 times larger than newly determined value by the potentiometric pH titration at $I = 0.1$ (NaClO₄).

(13) Shionoya, M.; Ikeda, T.; Kimura, E.; Shiro, M. *J. Am. Chem. Soc.* **1994**, *116*, 3848–3859. The Zn^{II} complexation constant $\log K(\text{ZnL})$ for **12a** is 15.1 ± 0.1 at 25 °C and $I = 0.10$ (NaClO₄). Kimura, E. and Ikeda, T. unpublished results.

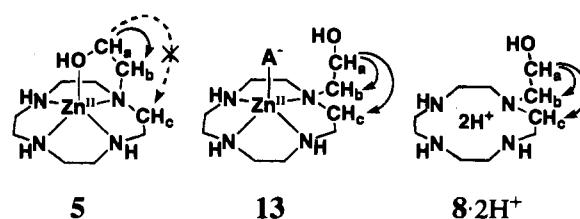


Figure 4. Proposed structures of **5**, the anion-bound complex **13** and two-protonated ligand **8·2H⁺** with the observed NOE correlations upon irradiation of H_a at [total L] = 20 mM and 30 °C. **5**: pD = 6.5, H_a → H_b 13.0%, H_a → H_c < 1%. **13**: A⁻ = OH⁻ (pD = 11) H_a → H_b 10.9%, H_a → H_c 4.8%; A⁻ = SCN⁻ (0.1 M, pD = 6.5) H_a → H_b 8.2%, H_a → H_c 5.0%; A⁻ = Cl⁻ (1 M, pD = 6.5) H_a → H_b 8.6%, H_a → H_c 4.5%. **8·2H⁺** pD = 6.5, H_a → H_b 8.8%, H_a → H_c 2.3%.

of the pendant alcohol would allow the greater NOE interaction between H_a and H_c. Similar NOEs for H_a → H_c were detected for the SCN⁻ and Cl⁻ anion complexes **14** (20 mM **5** and 0.1 M NaSCN or 1.0 M NaCl) and for the diprotonated **8·2H⁺** species at pD 6.5. In **14** the coordination of anion A⁻ should serve to shorten the distance between the pendant H_a and cyclen H_c. We tested a similar anion replacement reaction with the alcohol-pendant [12]aneN₃ complex **2a**. However, addition of a large excess A⁻ anion resulted in partial decomposition of the ZnL complex.

X-ray Crystal Structure of the Phosphate-Bound Zn^{II} Complex (ZnL-O-)₃P=O, 15. In order to isolate the monodeprotonated complex for the structural identification of ZnL-OH⁻ **11**, **5** was recrystallized from an aqueous alkaline solution (pH 9.5) in the presence of excess PF₆⁻ as a counter anion. The elemental analysis (C, H, N) and NMR (¹H, ¹³C, ³¹P) data of the precipitated crystals, however, suggested an unexpected formula (ZnL)₃PO₄(PF₆)₃ (**15**·(PF₆)₃). Apparently, PO₄³⁻ anion came from partial hydrolysis of PF₆⁻. Later, for better yield of this trimeric complex, we added K₂HPO₄ and NH₄PF₆ to **5** in pH 9.5 aqueous solution. The concrete evidence for the phosphate-coordinating trimeric structure, **15**·(PF₆)₃·(H₂O)_{1.5}, came from the subsequent X-ray crystal analysis. Since the pK_a value for HPO₄²⁻ ⇌ PO₄³⁻ + H⁺ is 11.7 (higher than 7.6 for the Zn^{II}-bound water of **5**) at 25 °C and $I = 0.1$,¹⁴ the ZnL complex should obviously have promoted the dissociation of a proton from HPO₄²⁻ by the strong binding of the resulting PO₄³⁻ with ZnL. In connection with the anion complexes ZnL-A⁻, the most basic PO₄³⁻ (next to OH⁻) must have a very strong affinity for the acidic Zn^{II}.¹⁵

Figure 5 shows an ORTEP drawing of the trimeric part **15** with 30% probability thermal ellipsoids. Crystal data and data collection parameters are displayed in Table 2. The phosphate PO₄³⁻ anion has replaced the pendant alcoholic OH and is centrally bound by three ZnL complexes. In the trimeric complex **15** there are three [ZnL]²⁺ ions around a 3-fold axis being through the phosphate P=O bond (see Figure 6). This is a novel synthetic trinuclear zinc complex solely bridged by inorganic phosphate PO₄³⁻.¹⁶

Each Zn^{II} ion is surrounded in a distorted tetragonal-pyramidal environment by the four nitrogen atoms (N₁, N₄, N₇, and N₁₀) and phosphate oxygen (O_{2p}). The structure of the monomeric

(14) Smith, R. M.; Martell, A. E. *Critical Stability Constants*; Plenum Press: New York, 1976; Vol. 4, p 56.

(15) Due to the complicate anion complexation between **5** and phosphate (e.g., ZnL-HPO₄²⁻, ZnL-PO₄³⁻, ZnL-PO₄³⁻-ZnL, etc.), the 1:1 anion affinity of **5** for PO₄³⁻ anion could not be determined by potentiometric pH titration.

(16) In biological systems several trinuclear zinc complexes are known at the active sites of Zn^{II}-containing phosphatases such as phospholipase C (Hough, E.; Hansen, L. K.; Briknes, B.; Jynge, K.; Hansen, S.; Hordvik, A.; Little, C.; Dodson, E.; Derewenda, Z. *Nature* **1989**, *338*, 357–360) and P1 nuclease (Volbeda, A.; Lahm, A.; Sakiyama, F.; Suck, D. *EMBO J.* **1991**, *10*, 1607–1618).

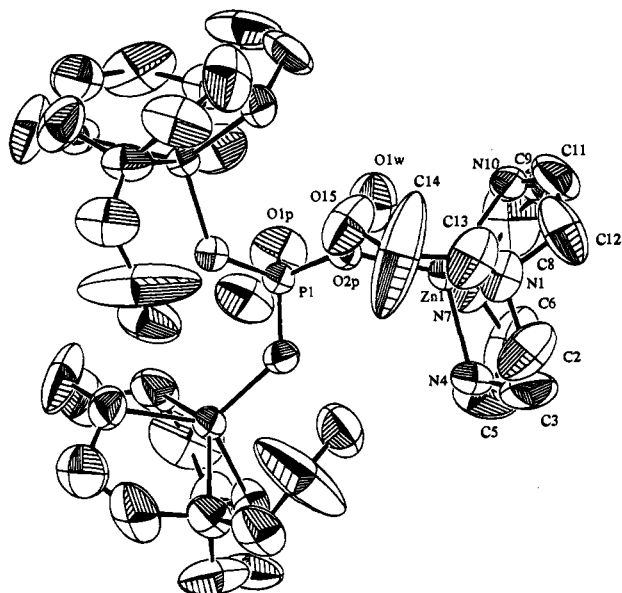


Figure 5. An ORTEP drawing (30% probability ellipsoids) of **15**-(PF₆)₃·(H₂O)_{1.5}. All hydrogen atoms and PF₆⁻ anions are omitted for clarity: Zn–O(2p) 1.920 (6), Zn–N(1) 2.238 (9), Zn–N(4) 2.084 (9), Zn–N(7) 2.13 (1), Zn–N(10) 2.097 (8) Å.

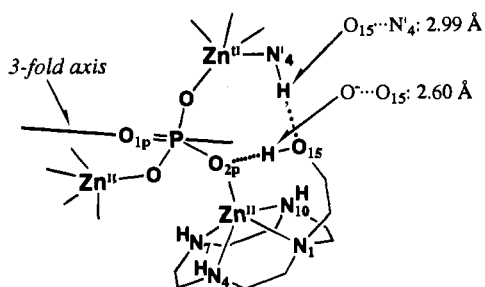


Figure 6. Hydrogen bonds in the trimeric complex **15** with the 3-fold axis.

ZnL part in **15** is similar to that of **5**. The zinc atom lies almost in a plane defined by the N₄, N₁₀, and O_{2p} atoms (a total angle for N₄–Zn–N₁₀, N₁₀–Zn–O_{2p}, and O_{2p}–Zn–N₄ is 359.9°). The angles N₁–Zn–N₇ and N₄–Zn–N₁₀ are bent at 137.9(4) and 131.7(4)°, respectively. A significant finding is a strong hydrogen bonding between the pendant OH group and phosphate O⁻ anion (O₁₅···O_{2p}, 2.60 Å), which may contribute to the stability of the phosphate Zn^{II} complex and polarize the neutral alcoholic OH group. The anionic phosphate O_{2p}–Zn bond length (1.920 Å) is shorter than that of the neutral alcoholic oxygen O₁₅–Zn in **5** (1.994 Å), supporting stronger interaction between the phosphate O⁻ donor and Zn^{II}.¹⁷

Thus, the pendant OH in **5** is pushed out from the first coordination sphere by the phosphate anion (see Figure 6). We failed to isolate the target complex **11** using various other counter anions.

Hydrolysis of 4-Nitrophenyl Acetate (NA) with the Alcohol-Pendant Cyclen–Zn^{II} Complex 5. The ZnL complex **5** has been tested as a model for a zinc site in alkaline phosphatase. Since the phosphomonoesters (e.g., 4-nitrophenyl phosphate) underwent extremely slow hydrolysis with **5** as with **1** and **4**,^{4d} we have resorted to carboxyester 4-nitrophenyl acetate (NA) hydrolysis at *I* = 0.10 (ca. 90 mM NaNO₃) and pH 6.4–9.5 (20 mM Good's buffers). Because NA is insoluble in pure

(17) Similar short Zn–O⁻(phosphate) bonds were reported for HPO₄²⁻-carboxypeptidase A (1.9 Å) (Mangani, S.; Ferraroni, M.; Orioli, P. *Inorg. Chem.* **1994**, *33*, 3421–3423) and PO₄³⁻ alkaline phosphatase complexes (1.97 Å) in ref 7b.

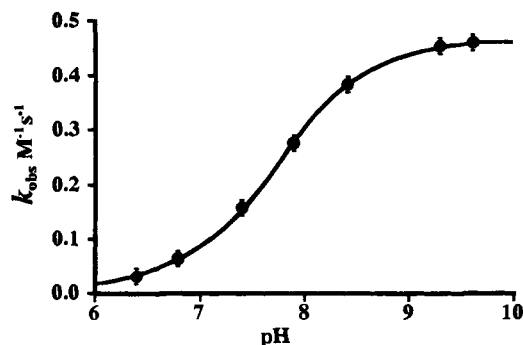
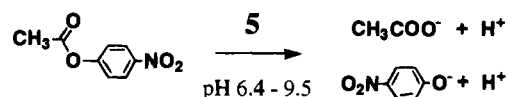


Figure 7. pH-rate profile for the first-order rate constants of 4-nitrophenyl acetate (NA) hydrolysis with 1 mM of alcohol-pendant cyclen–Zn^{II} complex (**5** and **11**) at 25 °C and *I* = 0.10 (NaNO₃) in 10% (v/v) CH₃CN.

Scheme 7



water, we selected CH₃CN as a cosolvent (10% (v/v)). The hydrolysis was followed by the appearance of 4-nitrophenolate at 400 nm (see Scheme 7), as previously done by **1b**,^{4a} **2b** (Scheme 2),⁶ and **4b**.⁹

The second-order dependence of the rate constant on the total concentration of Zn^{II} complex ([**5**] + [**11**]) and [NA] fits to the kinetic eq 7, where ν_{Zn} is the hydrolysis rate promoted by the active Zn^{II} complex. The observed rate constant, k_{obs} is plotted as a function of pH (see Figure 7). The resulting sigmoidal curve indicating characteristic of a kinetic process controlled by an acid–base equilibrium exhibits an inflection point at pH 7.7, which is identical to the pK_a value for the coordinate water of **5** independently measured by potentiometric pH titration in 10% (v/v) CH₃CN. Therefore, the reactive species is concluded to be the monodeprotonated species, most likely **11**, as discussed above. With the pendant-less cyclen complex, the monodeprotonated ZnL–OH⁻ **4b** was also the reactive species.⁹ The second-order rate constant k_{NA} for **11** (see eq 8) of 0.46 ± 0.01 M⁻¹ s⁻¹ was determined from the k_{obs} values at 25 °C. Since the initial k_{NA} value holds after more than one catalytic cycle (see Experimental Section), the hydrolysis is concluded to be catalytic.

$$\nu_{Zn} = k_{obs}[\text{total Zn}^{II} \text{ complex}][\text{NA}] \quad (7)$$

$$= k_{NA}[\mathbf{11}][\text{NA}] \quad (8)$$

For another reference, the NA hydrolysis catalyzed by the similarly *N*-monosubstituted cyclen complex, Zn^{II}–*N*-methylcyclen **12** has also been determined by the same method. The kinetics followed the second-order dependence on [NA] and [monodeprotonated species **12b**]. The rate constant k_{NA} value is $(4.7 \pm 0.1) \times 10^{-2}$ M⁻¹ s⁻¹ at 25 °C and *I* = 0.10 (NaNO₃). The comparison of the k_{NA} values (at 25 °C) for **11** and **12b** clearly demonstrates the 10 times more efficient catalysis by **11**. However, a question with **11** remained, which is the nucleophile to attack NA to yield 4-nitrophenolate, the Zn^{II}–OH⁻ or pendant alcoholic OH?

Intervention of an Acyl-Intermediate 16 in the NA Hydrolysis. The NA hydrolysis (Scheme 7) was followed by ¹H NMR with **5** (2 mM) and NA (2 mM) in buffered 10% (v/v) CD₃CN solution at pD 9 (0.1 M borate buffer) at 30 °C. The disappearance of the reactant NA signals (δ 2.39 (CH₃), 7.41 and 8.36 (ArH)) matched the appearance of the product

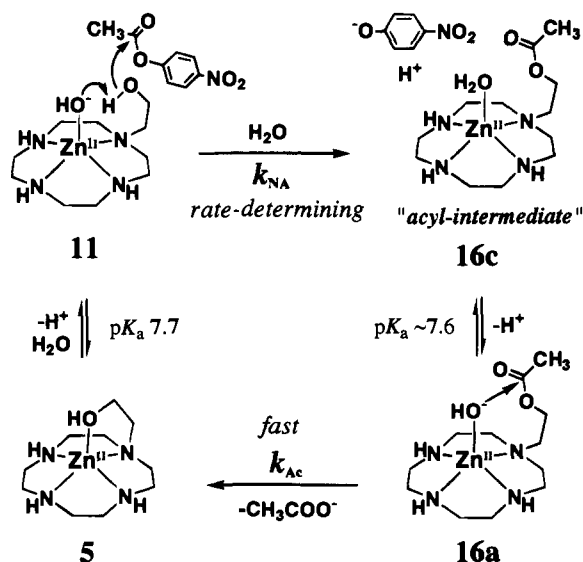
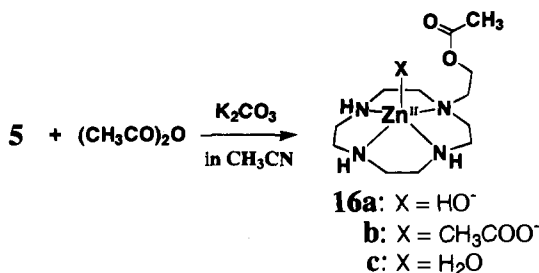


Figure 8. An overall reaction mechanism for NA hydrolysis catalyzed by alcohol-pendant cyclen-Zn^{II} complex.

CH₃COO⁻ (δ 1.91) and 4-nitrophenolate (δ 6.52 and 8.07). This confirmed that we have rightly followed the kinetics of the complete NA hydrolysis. On the other hand, a ¹H NMR study of the NA hydrolysis in *nonbuffered* solution showed transient proton signals (δ 2.10 and 4.32, ca. 0.3 mM) ca. 5 min after mixing **5** (12 mM; δ 3.81, CH₂OH), NaOD (10 mM) and NA (10 mM) in 10% (v/v) CD₃CN/D₂O solution at 30 °C, which have been assigned respectively to the methyl and methylene protons of a transient intermediate **16** (see next paragraph and Figure 8). Any other side product was not detected. In nonbuffered solution, the pH is lowered, as the reaction progresses (see Figure 8), where **16** barely survived. These results indicate that in the course of the catalytic NA hydrolysis by **11** the "acyl-intermediate" **16a** was initially formed, which immediately disappeared at neutral and alkaline pH to give the final hydrolysis products CH₃COO⁻ and the starting **11**.

The presumed acetate-pendant complex **16** was independently synthesized by treating **5**·(ClO₄)₂ with acetic anhydride (Scheme 8). The crystalline complex **16** was obtained as its CH₃COO⁻ and ClO₄⁻ salts. Since CH₃COO⁻ anion has a small but finite anion affinity for Zn^{II}-cyclen complexes (see Table 4), the complex in solid state may have a [CH₃COO⁻-ZnL]·ClO₄ formula **16b**, where CH₃COO⁻ ion is a ligand at the apical site and ClO₄⁻ a counteranion. The acetate pendant group in the complex **16b** showed the carbonyl stretching ν_{CO} (KBr pellet) at an ordinary wave number 1726 cm⁻¹,¹⁸ indicating that the ester carbonyl oxygen remains uncoordinated. The crystalline complex **16b** was found barely stable in acidic solution but unstable in neutral to alkaline aqueous solution, as shown by the very fast disappearance of the pendant acetate

Scheme 8



(18) (a) Collman, J. P.; Kimura, E. *J. Am. Chem. Soc.* **1967**, *89*, 6096–6103. (b) Alexander, M. D.; Busch, D. H. *J. Am. Chem. Soc.* **1966**, *88*, 1130–1138.

Table 4. A Comparison of Hydrolysis Rate Constants, k_{NA} (M⁻¹ s⁻¹) for **11**, **4b**, **12b**, **1b**, and **2b**, and Aqueous OH⁻ Ion at $I = 0.10$ (NaNO₃) and 25 °C in 10% (v/v) CH₃CN

catalyst	k_{NA}	catalyst	k_{NA}
11	0.46 ± 0.01 ^a	1b	3.6 × 10 ^{-2d}
4b	0.10 ^b	2b	0.14 ^d
12b	(4.7 ± 0.1) × 10 ^{-2c}	OH ⁻ _{aq}	8.1 ^b

^a Determined with 0.5, 1, and 2 mM **5**. ^b From ref 9. ^c Determined with 0.5, 1, and 2 mM **12b**, and 0.05, 0.1, and 0.2 mM NA at pH 9.3 (20 mM CHES buffer). ^d From ref 6.

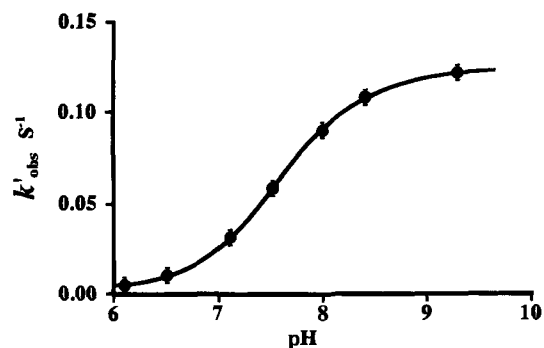


Figure 9. pH-rate profile for the first-order rate constants of intramolecular acetate hydrolysis of acetate-pendant cyclen-Zn^{II} complex (**16**) at 25 °C and $I = 0.10$ (NaNO₃) in 10% (v/v) CH₃CN.

group on ¹H NMR spectra. In neutral to alkaline pH solution, the acetate would be replaced by H₂O (**16c**) or OH⁻ (**16a**), since OH⁻ has much stronger affinity for Zn^{II}-cyclen complexes than CH₃COO⁻, see Table 3. The final product was proven to be CH₃COO⁻ and **5** (or **11**).

The hydrolysis rate (ν) of the acetate-pendant in **16** was followed by the evolution of H⁺ released from the product acetic acid, which was detected on spectral change of the appropriate pH-indicators at pH 6.1–9.3, $I = 0.10$ (NaNO₃) and 25 °C in 10% (v/v) CH₃CN using a rapid injection device. The first-order dependence on the total concentration of the ZnL complex (**16**) at various pH is consistent with the kinetic eq 9. The first-order rate constants, k'_{obs} , are plotted as a function of pH in Figure 9. The sigmoidal curve is characteristic of a kinetic process controlled by an acid-base equilibrium and exhibit an inflection point at pH 7.6, which is almost the same pK_a value as those for the coordinate waters of Zn^{II}-cyclen **4a** ($pK_a = 7.9$) and Zn^{II}-*N*-methylcyclen **12a** ($pK_a = 7.7$). Therefore, the reactive species is concluded to be the Zn^{II}-OH⁻ complex **16a**, in which the Zn^{II}-bound OH⁻ must be a good nucleophile to attack intramolecularly at the acetate pendant. Thus the first-order rate constant k_{Ac} of 0.12 ± 0.01 s⁻¹ was determined from the maximum k'_{obs} value at 25 °C and $I = 0.10$ (NaNO₃) (eq 10).

$$\nu = k'_{obs}[\text{total ZnL complex } \mathbf{16}] \quad (9)$$

$$= k_{Ac}[\mathbf{16a}] \quad (10)$$

The hydrolysis of the (otherwise "inactive") alkyl ester by the intramolecular Zn^{II}-OH⁻ is ca. 4000 times as fast as the intermolecular hydrolysis of the "active ester" 4-nitrophenyl acetate at [11] = 1 mM. This is reasoned by an extremely efficient proximal effect of the Zn^{II}-OH⁻. Similar proximal effect of the metal-bound OH⁻ has been well demonstrated with Co^{III},^{10,19} Cu^{II},²⁰ La^{III},²¹ etc.

We thus can draw an overall reaction mechanism as in Figure 8. The rate limiting step is the initial acyl migration from the substrate NA to the pendant alcohol. A half-life time of the first acyl transfer reaction with 1 mM **11** is 26 min, to be compared with 6 s for the second reaction under the same conditions.

A Comparison of NA Hydrolysis by Various Zn^{II}-Activated Nucleophiles. The NA hydrolysis rate constants with ZnL-OH⁻ complexes **11**, **4b**, **12b** and **1b**, ZnH₂L **2b**, and free OH⁻ ion are compared in Table 4. The NA hydrolysis with *N*-methylcyclen complex **12b** is approximately half as fast as with cyclen complex **4b**. The basicity of the Zn^{II}-OH⁻ complexes is nearly the same (pK_a = 7.7 and 7.9, respectively), so that the steric hindrance by the methyl substituent is probably responsible for the slower rate. Although the basicity of the ZnL-bound OH⁻ is almost the same for **11** and **12b**, the alcohol-pendant cyclen complex **11** reacts 10 times faster. Along with the evidence for the acyl-intermediate formation, this implies that *it is the pendant alcoholic (neutral) OH and not the Zn^{II}-OH⁻ that is a more powerful nucleophile.* The Zn^{II}-OH⁻ in **11** rather serves to activate the adjacent alcoholic OH. In other words, the function of Zn^{II}-OH⁻ as a nucleophile probably gives way to the role of general base to make up a dyad for the initial attack at the external electrophilic center. In the second reaction, however, the Zn^{II}-OH⁻ acts as a nucleophile by itself to attack the intramolecular acetate.

The strong nucleophilicity of the neutral alcohol OH in **11** may suggest a new mechanism of alkaline phosphatase, in which the alcoholic Ser(102) OH nucleophile is activated by the strong hydrogen bond with the Zn^{II}-bound OH⁻ at the active center to attack a substrate phosphomonoester. A conventional mechanism of alkaline phosphatase is that the serine alkoxide anion (bound to the Zn^{II}) directly attacks as a nucleophile at phosphomonoesters (Scheme 3).^{7a} Our earlier model with the alcohol-pendant [12]aneN₃ **2b** might mimic the latter mechanism.⁶ Just as the alkoxide anion complex **2b** reacts approximately four times faster than the corresponding hydroxo complex **1b** in N₃ macrocyclic system, the present neutral alcohol-pendant complex **11** reacts ca. five times faster than the hydroxo complex **4b** in N₄ macrocyclic system (see Table 4). These facts imply that alcoholic (e.g., serine) OH can be similarly a better nucleophile than H₂O whether it is activated either by direct (e.g., **2b**) or by indirect (hydrogen bonding with Zn^{II}-OH⁻, e.g., **11**) binding to Zn^{II}. The alcoholic OH group in zinc enzyme, which lies in the outer Zn^{II} coordination sphere thus may be activated by the Zn^{II}-OH⁻ general base.^{1,2,7b}

Summary and Conclusions

The novel alcohol-pendant cyclen **8** forms a stable 1:1 Zn^{II} complex ZnL²⁺ **5** with an apically binding neutral alcoholic OH at the fifth coordination site. The complex **5** has a dissociable proton with a pK_a value of 7.60 at 25 °C and *I* = 0.10 (NaClO₄). We conclude that the structure of the deprotonated species is a OH⁻-bound Zn^{II} complex **11**, rather than an alkoxide anion-bound complex **10** as reported for the alcohol-pendant [12]aneN₃ complex **2**. The pendant alcohol in **11** is activated by the adjacent general base Zn^{II}-OH⁻ and becomes a stronger nucleophile toward NA than the Zn^{II}-bound OH⁻. These results may be relevant to the activation mechanism of the nucleophilicity of the serine OH and other alcoholic groups in hydrolytic enzymes. Furthermore, in the course of NA hydrolysis with **11**, formation of an "acyl-intermediate" **16** was proven in the

rate-determining step. From the separate synthesis of **16** an extremely fast rate for the second reaction (half-life ca. 6 s) for **16a** (→ **11** + acetate) was established at pH 9.3, where a water is activated on Zn^{II}, and the resulting Zn^{II}-OH⁻ acts as a strong nucleophile to attack the intramolecular electrophilic center. We conclude that these results with the alcohol-pendant cyclen Zn^{II} complex **5** explain the intrinsic role of Zn^{II} in the alkaline phosphatase catalysis.

Experimental Section

General Information. All reagents used were of analytical reagent grade (purity >99%). The following pH-indicators and Good's buffers (Dojindo) were commercially available and used without further purification: chlorophenol red (pK_a = 6.3, Kishida Chem.), 4-nitrophenol (pK_a = 7.1, Nacalai Tesque), phenol red (pK_a = 7.5, Yoneyama Pharm.), metacrezol purple (pK_a = 8.3, Kishida Chem.), thymol blue (pK_a = 8.9, Yoneyama Pharm.); MES (2-(*N*-morpholino)ethanesulfonic acid, pK_a = 6.3), MOPS (3-(*N*-morpholino)-propanesulfonic acid, pK_a = 7.2), HEPES (*N*-1-hydroxyethylpiperazin-*N'*-2-ethanesulfonic acid, pK_a = 7.5), EPPS (*N*-2-hydroxyethylpiperazine-*N'*-3-propanesulfonic acid, pK_a = 8.0), TAPS (*N*-tris(hydroxymethyl)methylamino-propanesulfonic acid, pK_a = 8.4), and CHES (2-(cyclohexylamino)-ethanesulfonic acid, pK_a = 9.3). All aqueous solutions were prepared using deionized and distilled water. Acetonitrile (CH₃CN) was distilled over calcium hydride and stored in the dark. 4-Nitrophenyl acetate (NA) was recrystallized from dry diethyl ether.

Kinetic study was carried out by a visible spectral method using a Hitachi U-3500 spectrophotometer equipped with a thermoelectric cell temperature controller (±0.5 °C), a fast stirrer unit, and a rapid injection device RX1000 (Applied Photophysics). IR spectra were recorded on a Shimadzu FTIR-4200 spectrophotometer. Thin-layer chromatography (TLC) was carried out on Merck Art. 5554 (silica gel) TLC plate. ¹H (400 MHz), ¹³C (100 MHz), and ³¹P (162 MHz) NMR spectra were recorded on a JEOL α-400 spectrometer. 3-(Trimethylsilyl)propionic-2,2,3,3-*d*₄ acid sodium salt in D₂O and tetramethylsilane in organic solvent were used as internal references for ¹H and ¹³C NMR measurements. A D₂O solution of 80% phosphoric acid was used as an external reference for ³¹P NMR measurement.

Synthesis of 1-(2-Hydroxyethyl)-1,4,7,10-tetraazacyclododecane, **8.** 2,6-Dioxo-1,4,7,10-tetraazacyclododecane, **6** (3.0 g, 15 mmol),¹¹ was added dropwise to a DMF solution (300 mL) of ethyl bromoacetate (1.25 g, 7.5 mmol), followed by stirring at room temperature for 3 h. After the solvent was evaporated, the residue was dissolved in 20 mL of H₂O, and the solution was extracted with CH₂Cl₂ (80 mL × 13). After the organic layer was dried over anhydrous Na₂SO₄, the solvent was evaporated. The residue was crystallized from EtOH to obtain 10-((ethoxycarbonyl)methyl)-2,6-dioxo-1,4,7,10-tetraazacyclododecane (**7**) as colorless needles (1.35 g, 63% yield): mp 119.0–120.5 °C; IR (KBr pellet) 3357, 3320, 2980, 2934, 2853, 1734, 1645, 1545, 1447, 1418, 1370, 1358, 1325, 1275, 1179, 1082, 1030, 804, 691, 588 cm⁻¹; TLC (eluent; CH₂Cl₂/MeOH/28% aqueous NH₃ = 10:1:0.1) *R*_f 0.25; ¹H NMR (CDCl₃) δ 1.31 (3 H, t, *J* = 7.1 Hz, CH₃), 2.78 (4 H, m, NCH₂), 3.26–3.33 (4 H, m, NCH₂), 3.40 (2 H, m, NCH₂COO), 3.42 (4 H, s, NCH₂CON), 4.22 (2 H, q, *J* = 7.1 Hz, COOCH₂), 8.29 (2 H, br, CONH).

The dioxo macrocycle **7** (2.1 g, 7.3 mmol) was added to a solution of 10 times excess amount of BH₃-THF complex in 210 mL of dry THF at 0 °C. The solution was stirred at room temperature for 1 h and then heated at 60 °C for 1 day. After the excess amount of hydroborane complex was decomposed with water at 0 °C, the solvent was evaporated. The residue was dissolved into 150 mL of aqueous 6 M HCl, and then the solution was heated at 100 °C for 12 h. After the solvent was evaporated, the residue was passed through an anion exchange column (Amberlite IRA-400) with water to obtain **8** as a colorless oil. Crystallization of the oil from 6 M aqueous HCl afforded colorless needles as its tetrahydrochloride salts (**8**·4HCl·H₂O) in 66% yield: dec 228–230 °C; IR (KBr pellet) 3416, 2934, 2662, 1618, 1485, 1451, 1389, 1078, 1051, 1011, 959, 756, 570 cm⁻¹; ¹H NMR (D₂O) δ 2.80 (2 H, t, *J* = 5.2 Hz, NCH₂), 2.88–3.25 (16 H, b, NCH₂C), 3.70 (2 H, t, *J* = 5.2 Hz, CH₂O); ¹³C NMR (D₂O) δ 45.1, 45.3, 46.8, 52.0, 57.0, 60.5. Anal. Calcd for C₁₀H₃₀N₄O₄Cl₄: C, 31.6; H, 8.0; N, 14.7. Found: C, 32.0; H, 7.8; N, 14.9.

(19) Jones, D. R.; Lindoy, L. F.; Sargeson, A. M. *J. Am. Chem. Soc.* **1983**, *105*, 7327–7336.

(20) (a) Wahnou, D.; Hynes, R. C.; Chin, J. *J. Chem. Soc., Chem. Commun.* **1994**, 1441–1442. (b) Morrow, J. R.; Troglor, W. C. *Inorg. Chem.* **1988**, *27*, 3387–3394. (c) Groves, J. T.; Chamvers, Jr., R. R. *J. Am. Chem. Soc.* **1984**, *106*, 630–638. (d) Fife, T. H.; Bembi, R. *J. Am. Chem. Soc.* **1993**, *115*, 11358–11363.

(21) Hay, R. W.; Govan, N. *J. Chem. Soc., Chem. Commun.* **1990**, 714–715.

(22) Martel, A. E.; Motekaitis, R. J. *Determination and Use of Stability Constants*, 2nd ed.; VCH: New York, 1992.

(23) Khalifah, R. G. *J. Biol. Chem.* **1971**, *246*, 2561–2573.

Synthesis of 1-(2-hydroxyethyl)-1,4,7,10-tetraazacyclododecane Zn(II) complex, 5·(ClO₄)₂. 8·4HCl (500 mg, 1.3 mmol) was dissolved in water (50 mL) and passed through an anion exchange column (Amberlite IRA-400) with water to obtain the free ligand **8** as a colorless oil. After the oil was dissolved in EtOH (50 mL), Zn(ClO₄)₂·6H₂O (470 mg, 0.13 mmol) was added in the solution. The solution was stirred at 60 °C for 1 h. After the solvent was evaporated, the residue was recrystallized from H₂O/EtOH to obtain colorless prisms as diperchlorate salts 5·(ClO₄)₂ in 52% yield: dec 228 °C; IR (KBr pellet) 3438, 3254, 2959, 2938, 1622, 1480, 1456, 1298, 1285, 1146, 1113, 1092, 1024, 988, 627 cm⁻¹; ¹H NMR (D₂O, pD = 6.6) δ 2.70–3.14 (16 H, m, NHC₂), 2.91 (2 H, t, *J* = 5.7 Hz, NCH₂CO), 3.82 (2 H, t, *J* = 5.7 Hz, CH₂O); ¹H NMR (D₂O, pD = 11) δ 2.72–3.10 (16 H, m, NCH₂), 2.83 (2 H, t, *J* = 5.7 Hz, NCH₂CO), 3.76 (2 H, t, *J* = 5.7 Hz, CH₂O); ¹³C NMR (D₂O, pD = 6.6) δ 45.8, 46.7, 48.3, 54.1, 56.2, 59.6. Anal. Calcd for C₁₀H₂₄N₄O₉Cl₂Zn: C, 25.0; H, 5.0; N, 11.7. Found: C, 24.9; H, 5.2; N, 11.7.

Preparation of 1-(2-hydroxyethyl)-1,4,7,10-tetraazacyclododecane-Zn^{II}-phosphate complex, 15·(PF₆)₃(H₂O)_{1.5}. 5·(ClO₄)₂ (104 mg, 0.22 mmol) was dissolved in 1.5 mL of water. K₂HPO₄ (13 mg, 0.08 mmol) and NH₄PF₆ (35 mg, 0.22 mmol) were added, and the solution pH was adjusted to 9.5. Colorless prisms of 15·(PF₆)₃(H₂O)_{1.5} were obtained by slow evaporation of the solvent in 65% yield: dec 228 °C; IR (KBr pellet) 3439, 3252, 3218, 2959, 2938, 1480, 1456, 1298, 1285, 1121, 1092, 1009, 988, 974, 843, 627, 559 cm⁻¹; ¹³C NMR (D₂O) δ 45.8, 46.7, 48.2, 54.0, 56.1, 59.5; ³¹P NMR (D₂O) δ -114.3 (PF₆⁻, septet, *J* = 708 Hz), 4.8 (PO₄³⁻). The water molecules in the crystals are easily removed at 1 mmHg pressure and room temperature. Anal. Calcd for C₁₀H₂₄N₄O_{14/6}P_{4/3}F_{6/2}Zn (water-less form): C, 26.2; H, 5.3; N, 12.2. Found: C, 26.4; H, 5.3; N, 12.2.

Synthesis of 1-(2-acetoxyethyl)-1,4,7,10-tetraazacyclododecane Zn^{II} complex, 16b·ClO₄. 5·(ClO₄)₂ (1.3 g, 2.7 mmol) was dissolved in CH₃CN (100 mL) in the presence of K₂CO₃ (0.70 g, 5.2 mmol). (CH₃CO)₂O (1.3 g, 13 mmol) was added dropwise to the solution, and stirring was continued for 12 h at room temperature. After the solvent and excess acetic anhydride were evaporated, the residue was dissolved in CH₃CN (5 mL) and insoluble K₂CO₃ was filtrated off. Ether (20 mL) was added to this solution to obtain 16b·ClO₄ as colorless needles in 80% yield: dec 132 °C; IR (KBr pellet) 3440, 3303, 2930, 1726, 1609, 1402, 1242, 1138, 1121, 1088, 1038, 988, 675, 627 cm⁻¹; ¹H NMR (CD₃CN) δ 1.83 (3 H, s, CH₃COO⁻), 2.01 (3 H, s, CH₃COO), 2.62–3.03 (17 H, m, NCH₂C and CNHC), 3.00 (2 H, t, *J* = 5.7 Hz, NCH₂CO), 3.25 (2 H, b, CNHC), 4.25 (2 H, t, *J* = 5.7 Hz, OCH₂C); ¹H NMR (10% (v/v) CD₃CN, pD = ca. 5) δ 1.98 (3 H, s, CH₃COO⁻), 2.10 (3 H, s, CH₃COO), 3.09 (2 H, t, *J* = 5.4 Hz, OCH₂C), 4.32 (2 H, t, *J* = 5.4 Hz, OCH₂C); ¹³C NMR (CD₃CN): δ 21.2, 23.3, 43.5, 44.7, 45.6, 51.4, 52.1, 60.8, 171.5, 178.5. Anal. Calcd for C₁₄H₂₈N₄O₈·ClZn: C, 34.9; H, 6.1; N, 11.6. Found: C, 34.9; H, 6.1; N, 11.4.

Crystallographic Study. Colorless prismatic crystals of 5·(ClO₄)₂ (0.30 × 0.30 × 0.20 mm) and 15·(PF₆)₃(H₂O)_{1.5} (0.30 × 0.20 × 0.10 mm) were used for data collection. The lattice parameters and intensity data were measured on a Rigaku AFC7R diffractometer with graphite monochromated Cu Kα radiation and a 12 KW rotating anode generator. The structure was solved by direct methods and expanded using Fourier techniques. The non-hydrogen atoms were refined anisotropically. Hydrogen atoms were included but not refined. The final cycle of full-matrix least-squares refinement was based on 2438 and 1695 observed reflections (*I* > 3.00σ(*I*)) to give *R* = 0.073 and 0.070, and *R*_w = 0.125 and 0.112, respectively. All calculations were performed using the teXsan crystal structure analysis package developed by Molecular Structure Corporation (1985 and 1992). Drawing of the ORTEP structures was carried out with the computer graphic system CAChe (Sony Tektronics Co.).

Potentiometric pH Titrations. The preparation of the test solutions and the calibration of the electrode system were described earlier.⁶ All test solutions (50 mL) were kept under an argon (>99.999% purity)

atmosphere at 15.0, 25.0, and 35.0 ± 0.1 °C. The potentiometric pH titrations were carried out at *I* = 0.10 (NaClO₄ or NaNO₃), where at least three independent titrations were always made. The calculation methods for ligand protonation constants (*K_n*), Zn^{II} complexation constant (*K*(ZnL)) and a distribution diagram for relative species concentrations as a function of -log[H⁺] using the computer program BEST²² were the same as described previously.⁶ The protonation constants *K_n* are defined as [H_{*n*}L]/[H_{*n-1*}L]a_{H⁺}, the 1:1 metal complexation constant *K*(ZnL) as [ZnL]/[Zn^{II}][L], and the deprotonation constant *K_a* as [ZnL-OH⁻]a_{H⁻}/[ZnL]. The used values of *K_w*' (= [H⁺][OH⁻]) and *f_{H⁺}* at 15, 25, and 35 °C were 10^{-14.15}, 10^{-13.79} and 10^{-13.48} and 0.827, 0.825 and 0.823, respectively. The pH value in 10% (v/v) CH₃CN aqueous solution at *I* = 0.10 (NaNO₃) and 25 °C was determined by subtracting 0.03 units from pH meter reading, where *K_w*' of 10^{-13.97} of *f_{H⁺}* of 0.85 were used.

Kinetic Procedure for Hydrolysis of 4-Nitrophenyl Acetate Catalyzed by ZnL-OH⁻ Species. The hydrolysis rate of 4-nitrophenyl acetate (NA) catalyzed by ZnL-OH⁻ species was measured by an initial slope method (following the increase in 400-nm absorption (log ε = 4.24) of released 4-nitrophenolate) in 10% (v/v) CH₃CN aqueous solution at 25.0 ± 0.5 °C, as previously described for **1b**-, **2b**-, and **4b**-catalyzed NA hydrolyses.^{4a,6,9} Solutions containing 20 mM Good's buffer (MES, pH 6.4; MOPS, pH 6.8; HEPES, pH 7.4; EPPS, pH 7.9; TAPS, pH 8.4; CHES, pH 9.3 and 9.5) were used, and the ionic strength was adjusted to 0.10 with NaNO₃ (ca. 90 mM). For the initial rate determination, the following typical procedure was employed. NA (0.1, 0.2, and 0.5 mM) and **11** (0.5, 1.0, and 2.0 mM) were mixed in the buffered solution. The UV absorption increase was recorded immediately and then followed until ca. 2% liberation of 4-nitrophenolate. The observed first-order rate constants *k_{obs}* (s⁻¹) were calculated from the decay. The values of *k_{obs}*/[OH⁻ species] gave the second-order rate constant *k_{NA}* (M⁻¹ s⁻¹). All the experiments were run in triplicate, and the tabulated data represent the average of these experiments. Rate constants were reproducible to ±5%. To check if the NA hydrolysis was recycling (catalytic), we followed the NA hydrolysis rate until 80% completion at [NA] = 2.0 mM and [**11**] = 0.5 mM with 20 mM CHES buffer (pH 9.3) using the absorption increase at 458 nm (log ε 3.18). The second-order rate constant for **11** was identical to the initial rate constant determined above.

Kinetic Procedures for Hydrolysis of Acyl-Intermediate 16. In the hydrolysis of acyl-intermediate **16** at pH > 6 (10 mM Good's buffer, 10% (v/v) CH₃CN), 25 °C and *I* = 0.10 (NaNO₃), 1 equiv of proton is to be released from the product acetic acid. At alkaline pH, rapid liberation (< 1 s) of 1 more equiv of proton was observed before the acetate hydrolysis possibly due to the deprotonation of the coordinate water of **16c**. An CH₃CN solution of 20 mM CH₃COOH was used for quantitative analysis of the released proton. The hydrolysis rate was followed by the "change in pH-indicator" method, in which pairs of buffers and indicators having nearly the same p*K_a* values are employed, as described by Khalifah.²³ Buffer pH (10 mM), pH-indicator concentration, and wavelength (λ_{max}) at which the reaction was monitored are as follows: pH 6.1 and 6.5 (MES), 40 μM chlorophenol red, 576 nm; pH 7.1 (MOPS), 40 μM 4-nitrophenol, 400 nm; pH 7.5 and 8.0 (HEPES), 20 μM phenol red, 560 nm; pH 8.4 (TAPS), 40 μM metacrezol purple, 579 nm; pH 9.3 (CHES), 40 μM thymol blue, 598 nm. A typical procedure for the kinetic experiment is as follows: After 25 μL of 20 mM acetyl intermediate **16** in dry CH₃CN was rapidly injected into 2.5 mL of a buffer solution, the absorption decrease was recorded, where the final buffer and CH₃CN concentrations were 10 mM and 10% (v/v), respectively. The reactions followed excellent first-order kinetics for ≥ 5 half-lives. The pH change of the reaction mixture was within 0.1. Since the deprotonation of the coordinated waters of Zn^{II}-cyclen complexes (20 mM **5** and 20 mM **4a**) is too fast (≤ 1 s) to be followed by this method, the observed absorption decay with **16** was due to the acetate-pendant hydrolysis. The rate constants, *k_{Ac}* (s⁻¹) were obtained by a log plot method (correlation coefficients > 0.99).

Acknowledgment. We are thankful to the Ministry of Education, Science and Culture in Japan for financial support by a Grant-in-Aid for Scientific Research (A) (No. 04403024) for E.K. and by a Grant-in-Aid for Encouragement of Young Scientists (No. 06857180) for T.K. NMR instruments and a computer graphic system (Sony Tektronix) in the Research

Center for Medicinal Molecule (RCMM) of Hiroshima University were used.

Supplementary Material Available: Tables of crystallographic parameters, atomic coordinates, equivalent isotropic temperature factors, anisotropic temperature factors, bond lengths, and bond angles for **5**·(ClO₄)₂ and **15**·(PF₆)₃(H₂O)_{1.5}

(14 pages); listing of observed and calculated structure factors for **5**·(ClO₄)₂ and **15**·(PF₆)₃(H₂O)_{1.5} (30 pages). This material is contained in many libraries on microfiche, immediately follows this article in the microfilm version of the journal, and can be ordered from the ACS; see any current masthead page for ordering information.

JA942936B